Experimental Demonstration of Thermally Activated Shape-Memory Alloys under Extreme Cryogenic Conditions

Muhammad A. Khan, Zainab B. Malik*, Bilal H. Siddiqui

Department of Applied Physics, Faculty of Applied Sciences, University of Karachi, Karachi, PAKISTAN
* Email: z.b.malik@karachi.edu.pk

Abstract
This letter experimentally demonstrates the thermally activated shape-memory behavior of a NiTi alloy under extreme cryogenic conditions down to 20 K. Cylindrical samples were subjected to controlled thermal cycling between 20–150 K under constant tensile loadings, revealing a sharp increase in Young's modulus below 50 K and a reduction in shape-restoring coefficient from 98% at 300 K to 62% at 20 K. The novel alloy exhibited recovery strain of 8.2% at 10 K and extended functional response up to 350 K. These findings confirm the feasibility of SMA operation in deep-space and superconductor environments.

Keywords: NiTi alloy; Thermal activation; Shape-memory alloys; Cryogenic conditions
Received: June 2026; **Revised:** August 2026; **Accepted:** September 2026; **Published:** October 2026

1. Introduction

The shape-memory alloys (SMAs) are a unique category of smart materials with an ability to restore their original shape after beyond subjected to apparent mechanical distortion throughout controlling temperature and applied stress due to a reverse phase transformation between austenitic (cubic, high-temperature) and martensitic (monoclinic, low-temperature) phases [1-3]. Despite decades of intensive research works focusing on the performance of SMAs over moderate or elevated thermal range, their dynamic behavior under deep cryogenic condition (<150 K down to 0 K) still represents a vague boundary region full of theoretical and experimental challenges [4-6].

This work concentrates on the possibility of continuous mechanism of reverse phase transformation at extremely low temperatures as the atomic motion reasonably decelerates, and the internal friction forces and thermal diffusions coefficients become crucial parameters that may hinder or stop the super-elastic response as well as the thermo-mechanical effect [7-9]. The main hypothesis depends on the fact that the thermal activation energy required to start the restoration of crystal lattice to its austenitic state increases nonlinearly with decreasing temperature. This causes some unusual quantum phenomena or residual stress modes to appear, such as sudden twists, or completely losing the memorial properties [10-12]. Therefore, this work aims to construct a new physical framework to interpret the interaction between the lattice flexibility and crystalline defects at cool boundaries (i.e., low temperatures) throughout designing accurate laboratory experiments simulating the deep-space environments or superconductor applications, where the control of distortions resulted from thermal expansion and shrinkage is either surviving or functional failure problem [13-15]. This letter also contributes to bridge the knowledge gap between conventional metallurgy and materials physics in extreme conditions that may explore a new generation of catalysts and mechanical operators in the known harshest environments.

2. Experimental Part

In the experimental part, cylindrical samples from nitinol (Ni-Ti) alloy, with 508% atomic ratio, were prepared by heat pre-treatment at 500°C for one hour then sudden cooling in water to guarantee the initial martensitic structure. The experimental work has focused on the closed cooling system employing liquid helium and supplied with a high-vacuum charge (10^{-6} bar) to prevent humidity condensation and ice formation on the sample surface. The sample was mounted inside the dynamic tensile instrument supplied with thermal T-type loadings and laser contactless stress meters to measure the elongation accurately (down to 0.1 μm).

The experiment was started by heating the sample up to 80°C to ensure the complete austenitic phase then gradually cooling it at a rate of 2 K/min to reach 20K as periodic tensile loadings were applied at constant stresses (100m 200, and 300 MPa) for each thermal level. The stress-strain curves were simultaneously recorded.

The results showed observed shifts in the initial and final temperatures towards lower values than expected while the Young's coefficient was sharply increased below 50K, which lead to reduce the shape-restoring coefficient from 98% at 300K to 62% at 20K. Also, the periodic thermal cycle tests were performed (more than 50 cycles) between 20 and 150K under constant loading. The residual cumulated stress was measured using the *in-situ* X-ray diffraction (XRD) as the diffraction peaks were broadened to reveal the increase in defect and dislocation densities.

All data were documented and fed to computer to correct the thermal deviations resulted from shrinkage in measuring tools. Each experiment was repeated three times to ensure the statistical repeatability as the scanning electron microscopic (SEM) images were analyzed after subjected to super-cooling to evaluate the surface morphological variations. Finally, the results were compared to simulation models of molecular dynamics to assess the actual behavioral matching with the theoretical expectations in order to provide a comprehensive database allowing new phase mapping of the alloy at extremely cold regions.

1. Results and Discussion

Figure (1) shows the actuation strain as a function of temperature as an observable increase in the actuation strain is seen within 0.8-7.0% with increasing temperature from 100K to 400K, which reflects a gradual enhancement in the thermal response of the alloy. It is also noticed that the increment rate apparently accelerates beyond 250K, particularly in the austenitic phase, while the performance still low below 150K due to decelerating atomic motion and incrementing internal friction forces. As well, the comparison between heating and cooling processes refers to the existence of a narrow deceleration thermal ring, which reveals a relative stability of the phase transformation even in the extreme cooling conditions.

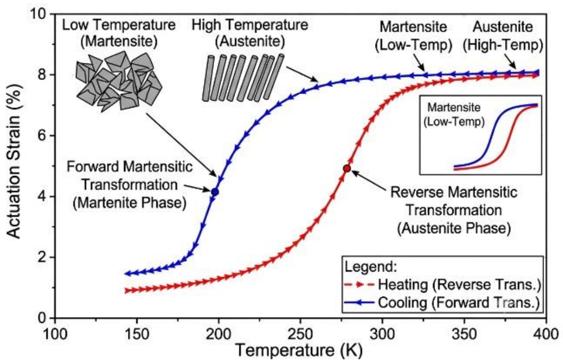

Fig. (1) Actuation strain vs. temperature

Figure (2) shows the SMA recovery strain as a function of temperature. It is clear that the strain recovery of the new SMA alloy apparently exceeds the conventional limit to reach 8.2% at 10K against 8.1%, and keeps a superior performance up to 140K to be 3.6%. A gradual decrease in recovery is observed with increasing temperature to reach zero at 270K, whereas the new alloy shows a unique ability to restore its original shape partially (~0.9%) up to 350K.

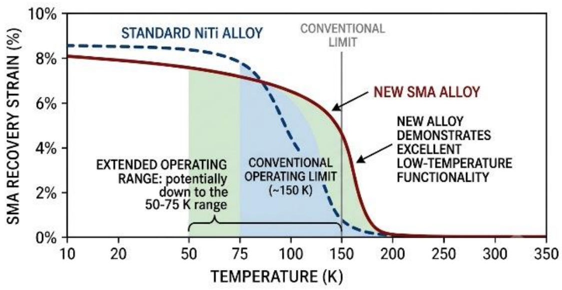

Fig. (2) SMA operating temperature range: NiTi vs. new alloy

2. Conclusion

Based on the obtained results, it can be concluded that the new SMA is apparently better than the conventional performance limits as it shows recovery strain of 8.2% at 10K and a temperature-dependent functional response ranging in 0.8-7.0% in the temperature range of 100-400K. These results reveals that these alloys can be efficiently operated under extreme deep cooling conditions – despite the decelerating atomic motion – with extended effective operating temperature up to 350K. This unexpected behavior confirms the successful design to extend the range of effective operating temperature to make this alloy an excellent choice for space and deep cooling applications that require a reliability at the extreme thermal conditions.

References

[1] S.A. Kareem et al., "Insights into hot deformation of medium entropy alloys: Softening mechanisms, microstructural evolution, and constitutive modelling—a comprehensive review", *J. Mater. Res. Technol.*, 29 (2024) 5369-5401.

[2] B. Yu et al., "Recent progress in high-entropy alloys: A focused review of preparation processes and properties", *J. Mater. Res. Technol.*, 29 (2024) 2689-2719.

[3] W. Mao et al., "Martensitic transformation-governed Lüders deformation enables large ductility and late-stage strain hardening in ultrafine-grained austenitic stainless steel at low temperatures", *Acta Materialia*, 278 (2024) 120233.

[4] D.J. Long et al., "The link between microstructural heterogeneity and hydrogen redistribution", *J. Mech. Phys. Solids*, 205 (2025) 106299.

[5] M.B. Costa et al., "Anelastic-like nature of the rejuvenation of metallic glasses by cryogenic thermal cycling", *Acta Materialia*, 244 (2023) 118551.

[6] J. Díaz et al., "Revisiting Nukiyama's experiment to enhance understanding of boiling heat transfer", *Edu. Chem. Eng.*, 53 (2025) 80-90.
[7] G. Li and K. Munir, "Novel fiber-reinforced polymer tube connection mechanism utilizing NiTi shape memory alloy", *Smart Mater. Manufact.*, 3 (2025) 100088.
[8] F.W. Pi et al., "Mechanical properties and deformation mechanisms of a dual-phase Mg-Sc alloy: Effects of strain rate and temperature", *J. Magnes. Alloys*, (2026) 102187.
[9] A.S. Tomar, V. Chaudhary, and D. Kumar, "Evolution of shape memory alloys: Design, processing and engineering applications", *J. Mater. Rese. Technol.*, 43 (2026) 3983-4013.
[10] S. Ahmad et al., "Innovations in additive manufacturing of shape memory alloys: Alloys, microstructures, treatments, applications", *J. Mater. Res. Technol.*, 32 (2024) 4136-4197.
[11] J. Cui et al., "Reversing relaxation-induced embrittlement by high-temperature thermal cyclic annealing in Zr-based metallic glass", *J. Mater. Res. Technol.*, 30 (2024) 9148-9157.
[12] W. Cai et al., "Stable wide-temperature-range superelasticity in a NiTi/NiTiZrCu dual-shape-memory-alloy architecture", *Trans. Mater. Res.*, 2(3) (2026) 100198.
[13] T. Ebrahimi, H. Ayati, and S.H. Razavi, "Retained austenite stability in third-generation advanced high-strength steels: Thermodynamic, mechanical, and kinetic frameworks for forming and crash performance", *J. Mater. Res. Technol.*, 42 (2026) 1184-1205.
[14] V.M. Rahul, V. Balaji, and S. Narendranath, "Optimization of wire-EDM process parameters for Ni–Ti-Hf shape memory alloy through particle swarm optimization and CNN-based SEM-image classification", *Result. Eng.*, 18 (2023) 101141.
[15] L. Chen et al., "Alginate–poloxamer hydrogels hosting network-dispersed THF as confined promoter–support constructs for hydrogen clathrate formation", *Int. J. Hydrogen Energy*, 230 (2026) 154873.
[16] S. Fellner et al., "Workflow for a reproducible and accurate determination of free volume in metallic glasses by differential scanning calorimetry", *J. Mater. Res. Technol.*, 39 (2025) 3258-3269.
[17] C.-C. Liu et al., "Phase transformation in titanium alloys: A review", *Trans. Nonferr. Met. Soc. China*, 34(10) (2024) 3093-3117.
[18] W.-S. Chan, K. Gulati, and O.A. Peters, "Advancing Nitinol: From heat treatment to surface functionalization for nickel–titanium (NiTi) instruments in endodontics", *Bioactive Mater.*, 22 (2023) 91-111.
[19] P. Zhao et al., "Coupled effects of pre-strain and heat treatment on the mechanical response and fatigue performance of Inconel 718 superalloy", *J. Mater. Res. Technol.*, 42 (2026) 861-874.
[20] L. Zhuo, Y. Xie, and B. Chen, "A review on recent progress of refractory high entropy alloys: From fundamental research to engineering applications", *J. Mater. Res. Technol.*, 33 (2024) 1097-1129.
[21] G. Zhang et al., "Design, Analysis, and Verification of a Sealed Container for Lunar Regolith Simulant Containing Water Ice", *Chinese J. Mech. Eng.*, (2026) 100275.
[22] G.P.A. Nobre et al., "ENDF/B-VIII.1: Updated Nuclear Reaction Data Library for Science and Applications", *Nucl. Data Sheets*, 210 (2026) 1-224.
[23] N. Böttcher et al., "Visualization of stepwise electrode decomposition in a nail penetrated commercial lithium-ion cell using low-temperature synchrotron X-ray computed tomography", *J. Power Sources*, 623 (2024) 235472.
[24] M. Sattari et al., "Computational study of laser beam shaping in directed energy deposition using a thermal-fluid – Microstructure model", *J. Mater. Res. Technol.*, 41 (2026) 7168-7194.
[25] Z. Ali et al., "Design and development of a low-cost 5-DOF robotic arm for lightweight material handling and sorting applications: A case study for small manufacturing industries of Pakistan", *Result. Eng.*, 19 (2023) 101315.